

Supplementary Information

A cyclic-triphosphazene based single-ion polymer electrolyte prepared via click reaction for lithium metal batteries

Kuan Lu,^a Cengliang Shan,^a Huinan Li,^a Hongbin Li,^a Hui Zhang,^a Chen Xiong,^a Wei Hu,^b Baijun Liu ^{*a}

^a Key Laboratory of High Performance Plastics of the Ministry of Education. National & Local Joint Engineering Laboratory for Synthesis Technology of High Performance Polymer. College of Chemistry, Jilin University, 2699 Qianjin Street, Changchun 130012, P. R. China.

^b Key Laboratory of Polyoxometalate Science of the Ministry of Education. Faculty of Chemistry, Northeast Normal University, 5268 Renmin Street, Changchun 130024, P. R. China.

1 Experimental

1.1 Materials

Oxalyl chloride (98%), 4-styrenesulfonic acid sodium salt (90%), trifluoromethylsulfonamide (98%), 4-dimethylaminopyridine (99%), 2,2-dimethoxy-2-phenylacetophenone (DMPA, 99%), hexachlorocyclotriphosphazene (HCCP, 98%), eugenol (99%), potassium carbonate (99%), LiTFSI (99.9%) and LiClO₄ (98%) were purchased from Aladdin. Pentaerythritol tetra(3-mercaptopropionate) (PETMP, 95%) was purchased from Sigma-Aldrich. Polyethylene glycol diacrylate (PEGDA, Mw=600), triethylamine (99.5%), acetonitrile (99.9%), N,N-Dimethylacetamide (DMAc, 99.8%) and N,N-dimethylpyrrolidone (99.9%) were purchased from energy chemical. LiFePO₄, Super P, PVDF and plasticizer (DMC:EC = 1:1 Vol% with 5% FEC) were purchased from Dodochem. All the chemicals were used as received.

1.2 Synthesis of hexa(4-allyl-2-methoxyphenyl) phosphazene (HEP)

According to a previously reported synthetic routine,¹ eugenol (4.2537 g, 25.9 mmol) was dissolved in 20 mL of anhydrous acetonitrile under a nitrogen atmosphere. Anhydrous potassium carbonate (5.3695 g, 28.8 mmol) was added to this solution, which was then mixed homogeneously by magnetic stirring at room temperature. Separately, HCCP (1.0000 g, 2.88mmol) was dissolved in 20 mL of anhydrous acetonitrile. This solution was then added dropwise to the eugenol/potassium carbonate mixture using a constant pressure dropping funnel. Following the complete addition of HCCP, the temperature of reaction mixture was increased to 85 °C. The reaction was allowed to proceed for 48 hours. Upon completion of the reaction, the mixture was filtered to remove insoluble parts. The filtrate was concentrated using vacuum rotary evaporation to yield the crude product. The crude product was recrystallized in ethanol and ultimately pure HEP was obtained. The yield was 85%.

¹H NMR (400 MHz, CDCl₃): δ 6.94 (d, 6H), 6.62 (d, 6H), 6.49 (dd, 6H), 5.91 (m, 6H), 5.11–5.04 (m, 12H), 3.66 (s, 18H), 3.30 (d, 12H).

1.3 Preparation of lithium (4-styrenesulfonyl) (trifluoromethanesulfonyl) imide

(LiSTFSI)

According to the a previously reported synthetic routine,^{2,3} sodium 4-styrenesulfonate (6.0000 g, 29.0 mmol) and N,N-dimethylformamide (0.1305 g, 1.5 mmol) were added to 60 mL of anhydrous acetonitrile and stirred to make a homogeneous mixture under nitrogen atmosphere. Oxalyl chloride (3 mL, 35 mmol) was added dropwise to the reaction mixture at 0 °C, followed by a reaction at room temperature for 24 h. The resulting sodium chloride precipitate was filtered out, and the acetonitrile solvent was removed by rotary evaporation to obtain 4-styrenesulfonyl chloride.

Under a nitrogen atmosphere, trifluoromethanesulfonamide (4.3385 g, 29.1 mmol), 4-dimethylaminopyridine (0.3152 g, 2.6 mmol), triethylamine (12.15 mL, 87.0 mmol) and 50 mL of anhydrous acetonitrile were added to a round-bottom flask and stirred until all reagents dissolved. 4-Styrenesulfonyl chloride was slowly added to the flask at 0 °C, and the mixture was reacted at room temperature for 20 h. Acetonitrile was removed by rotary evaporation, and the resulting viscous liquid was dissolved in dichloromethane (DCM). Subsequently, the mixture was washed with 40 mL of 4 wt% NaHCO₃ aqueous solution and 20 mL of 1.0 M HCl, resulting in a DCM solution containing (4-styrenesulfonyl)(trifluoromethanesulfonyl)imine. The DCM was then removed to obtain a brown liquid. The brown liquid was neutralized in distilled water with an excess of K₂CO₃ to ultimately obtain (4-styrenesulfonyl)(trifluoromethanesulfonyl) imine potassium (KSTFSI). The resulting suspension was stirred overnight at 0 °C, filtered, and vacuum-dried at 60 °C to obtain a light yellow solid. This solid was recrystallized in distilled water to yield a white high-purity KSTFSI powder (yield: 90%).

In a round-bottom flask, KSTFSI was dissolved in acetonitrile, and LiClO₄ was added dropwise to the above solution while stirring at room temperature overnight. KClO₄ was removed by filtration, and the filtrate was evaporated to obtain white solid LiSTFSI. The residual trace solvent was vacuum-dried overnight at 60 °C, and the product was stored in a glove box (H₂O, O₂ < 0.1 ppm) for further use (yield: 65%). The ¹H NMR spectrum of LiSTFSI is shown in the Figure S1.

¹H NMR (400 MHz; DMSO; ppm): δ 7.69 (d, 2H); 7.57 (d, 2H); 6.76 (q, 1H); 5.95 (d, 1H); 5.35 (d, 1H).

1.4 Preparation of single-ion crosslinked network polymer electrolytes (SICPEs)

PETMP (0.3 mmol), LiSTFSI (0.6 mmol) and DMPA (0.03 mmol) were added to a certain amount of DMAc and stirred to dissolve at room temperature, followed by irradiation under UV (365 nm) for 20 minutes to obtain a transparent solution. Then, HEP (0.1 mmol), PETMP (0.2 mmol) and PEGDA (0.4 mmol) were added to the DMAc and stirred to dissolve at room temperature. Subsequently, 1% mass ratio of DMPA was added to the solution, and after ultrasonic treatment for 5 minutes, the solution was poured into a polytetrafluoroethylene-mold and irradiated under UV (365 nm) for 30 minutes to obtain a crosslinked membrane soaked in solvent. The membrane was then dried in a vacuum oven at 100 °C for 48 hours to remove excess solvent, yielding the polymer electrolyte membrane (SICPE-4). Following the same steps, the SICPE membrane prepared with a molar ratio of HEP : PETMP : PEGDA600 = 1:1:2 was named SICPE-2 and the SICPE membrane prepared with a molar ratio of HEP : PETMP : PEGDA600 = 1:3:6 was named SICPE-6. During the preparation, the ratio of carbon-carbon double bonds to thiols was kept constant at 1:1. The thickness of the prepared electrolyte membranes are controlled to be ~150 μ m. When assembling the batteries, 30 μ L of plasticizer (DMC:EC = 1:1 Vol% with 5% FEC) was added to the obtained SICPE membrane.

1.5 Preparation of dual-ion crosslinked network polymer electrolytes (DICPEs)

HEP (0.1 mmol), PETMP (0.5 mmol), PEGDA600 (0.4 mmol) and of LiTFSI (0.6 mmol) were added to a certain amount of DMAc and stirred to obtain a uniform solution at room temperature. Then, 1% mass ratio of DMPA was added to the above solution. After ultrasonic treatment for 5 minutes, the solution was poured into a polytetrafluoroethylene mold and irradiated under UV (365 nm) for 30 minutes to obtain a crosslinked membrane soaked in solvent. The membrane was then dried in a vacuum oven at 100 °C for 48 hours to remove excess solvent, yielding the polymer electrolyte membrane DICPE-4. When assembling the battery, 30 μ L of plasticizer (DMC:EC = 1:1 Vol% with 5% FEC) were added to the obtained DICPE membrane.

1.6 Preparation of cathode electrode and assembly of battery

A mixture of LiFePO₄ (80 wt.%), super P (10 wt.%) and PVDF (10 wt.%) was thoroughly stirred in N,N-dimethylpyrrolidone to obtain the cathode electrode slurry. The slurry was cast on an aluminum foil using a coating rod and vacuum-dried at 120 °C for 12 h. The dried cathode electrode was cut into discs with a diameter of 12 mm and stored in a glove box for later use. The thickness of the LFP anode film was strictly kept at 40 μ m during preparation. And the active mass loading is \approx 1.5 mg cm⁻². The lithium metal anode was purchased from China Energy Lithium Co., Ltd, with a thickness of 0.45 mm and a diameter of 15.6 mm. The prepared cathode electrode, lithium metal anode electrode and SICPEs were assembled into a 2025 type coin cell battery of LiFePO₄/SICPEs/Li to test its cycling performance and rate capability.

2 Material characterizations of polymer electrolytes (PEs)

The chemical structure of the products was analyzed using a 400 MHz Bruker Advance III nuclear magnetic resonance (NMR) spectrometer. ¹H NMR spectroscopy was conducted at room temperature. FT-IR spectroscopy spectra were obtained from a Nicolet Impact 410 Fourier Transform Infrared spectrometer recorded from 4000 to 400 cm⁻¹ at room temperature. Thermogravimetric analysis (TGA) was performed using a Mettler Toledo TGA2, under a nitrogen atmosphere, with a temperature range of 100 to 600 °C and a heating rate of 10 °C min⁻¹. The microstructure of the samples was characterized using a Nova nano 450 field emission scanning electron microscope from FEI Company, with gold sputtering treatment applied prior to sample observation. The mechanical properties of the membranes were measured using a Shimadzu AG-1 testing machine at a strain rate of 1 mm min⁻¹. Differential scanning calorimetry (DSC) was conducted using a Q2000 differential scanning calorimeter from TA Instruments, with nitrogen protection during the measurement, covering a temperature range of -80 to 100 °C and a heating rate of 10 °C min⁻¹.

3 Electrochemical characterizations of PE

Ionic conductivity was obtained from stainless steel SS/SICPE-4/SS configuration cells by electrochemical impedance spectroscopy (EIS) using the electrochemical

chemical station. EIS was conducted from 10^6 to 0.1 Hz and amplitude of 10 mV in different temperatures. The ionic conductivity was calculated by the Equation $\sigma = L/R \times S$, where σ ($S\text{ cm}^{-1}$) is the ionic conductivity, L is the thickness of the sample, R refers to the resistance value tested by EIS, and S represents the contacting area of the SS and SPE.

Linear sweep voltammetry (LSV) is used to determine the electrochemical stability window of the electrolyte by assemble SS/SICPE-4/Li batteries. SS acts as the working electrode and the lithium foil serves as reference electrode. The measurement range is from 0 to 6 V (vs. Li^+/Li) with a scan rate of 1 mV s^{-1} at $25\text{ }^\circ\text{C}$.

Using the chronoamperometry (CA) method to determine the lithium ion transference number (t_{Li^+}) by assemble Li/SICPE-4/Li batteries. The calculation formula is as follows:

$$t_{\text{Li}^+} = I_0 (\Delta V - I_s R_s) / I_s (\Delta V - I_0 R_0)$$

Where ΔV is the polarization voltage applied during testing, I_0 and I_s are the initial and steady-state currents, while R_0 and R_s are the initial and steady-state resistances, respectively. The applied polarization voltage for this experiment is 10 mV, and the testing frequency ranges from 10^6 Hz to 0.1 Hz.

The Li/SICPE-4/Li symmetric batteries were cycled for stripping and deposition at $25\text{ }^\circ\text{C}$, with each step lasting 1 hour. Following the cycling of the symmetric lithium batteries, they were disassembled within argon-filled glove box. After cycling the battery, the lithium foils were removed in the glove box, subsequently cleaned with anhydrous dimethyl carbonate (DMC) and the surface morphology was observed using scanning electron microscopy (SEM).

To assess the electrochemical performance of PE, LiFePO_4 /SICPE-4/Li batteries were evaluated for rate capability at current densities ranging from 0.1 to 2 C (1 C = 170 mAh g^{-1}). Both rate capability and cycling performance tests were conducted at a temperature of $25\text{ }^\circ\text{C}$ and within a voltage range of 2.5 to 4.0 V.

Table S1. Compositions of cross-linked polymer electrolytes

Crosslinking section (mmol)	HEP	PETMP	PEGDA	LiSTFSI	LiTFSI
SICPE-2	0.1	0.4	0.2	0.6	0
SICPE-4	0.1	0.5	0.4	0.6	0
SICPE-6	0.1	0.6	0.6	0.6	0
DICPE-4	0.1	0.5	0.4	0	0.6

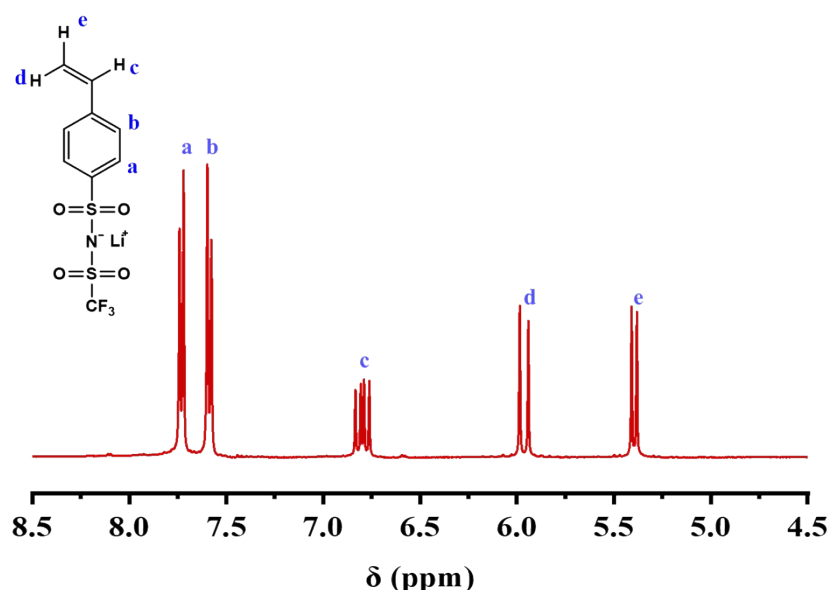


Fig. S1. ^1H NMR spectrum of the prepared LiSTFSI.

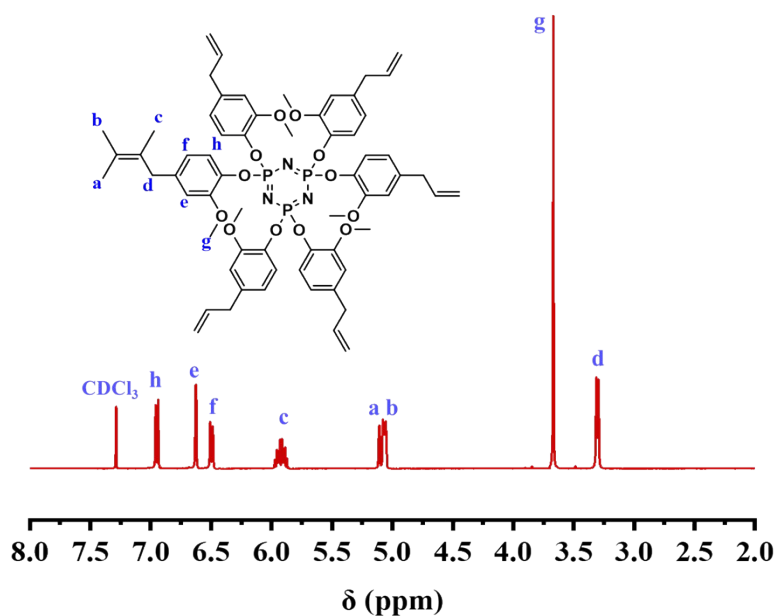


Fig. S2. ¹H NMR spectrum of the prepared HEP.

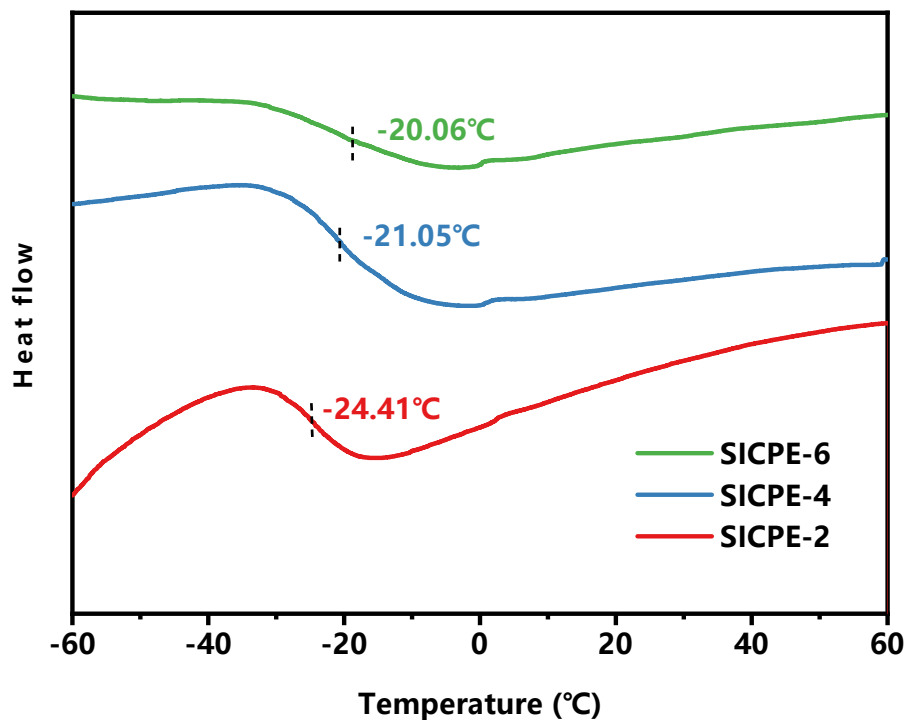


Fig. S3. DSC curves of the SICPE series.



Fig. S4. Combustion experiments of (a) the PP separator and (b) the SICPE membrane.

A combustion test was conducted to evaluate the flame-retardant properties of PP separator and the SICPE membrane. The PP separator and SICPE-4 electrolyte membrane were ignited using an ignition gun, and the combustion phenomena of the two samples were observed. The PP separator shown in Fig. S4a shrinks and rolls up immediately after contact with the flame and is extremely easy to ignite. In contrast, as shown in the Fig. S4b, when the flame approached the SICPE membrane, no significant shrinkage occurred. Due to the presence of a cross-linked network of cyclic-triphosphazene, the SICPE membrane was difficult to ignite, and the shape of the samples did not change significantly after the flame was withdrawn. This is primarily attributed to the stable three-dimensional cross-linked network in the SICPE and the inherent flame-retardant properties of the cyclic-triphosphazene networks.

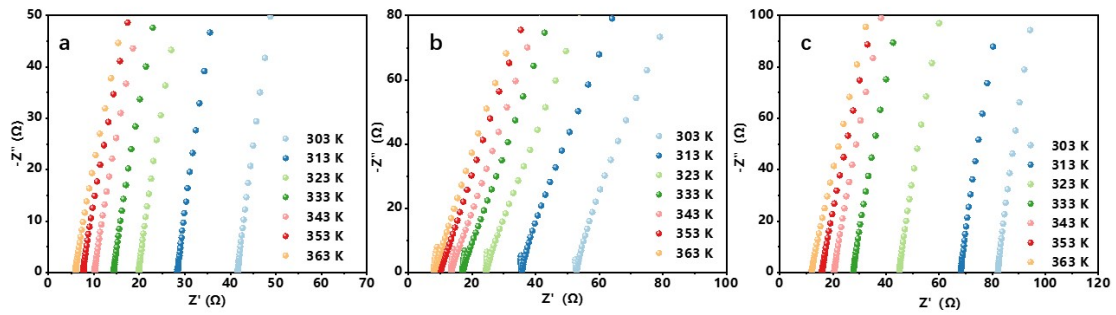


Fig. S5. EIS of (a) SICPE-2, (b) SICPE-4, and (c) SICPE-6 from 30 to 90 °C.

Table S2. Resistance and ionic conductivity of SICPEs at different temperatures

(thickness of $\sim 150 \mu\text{m}$)

Temperatur e (°C)	Impedance (Ω)			Ionic conductivity ($10^{-4} \text{ S cm}^{-1}$)		
	SICPE-2	SICPE-4	SICPE-6	SICPE-2	SICPE-4	SICPE-6
30	34.26	52.90	82.19	2.23	1.48	0.74
40	24.41	35.77	68.21	3.14	2.18	1.12
50	18.36	24.51	45.06	4.17	3.18	1.70
60	13.70	17.22	27.79	5.59	4.53	2.75
70	11.11	13.56	20.60	6.89	5.76	3.72
80	9.10	10.16	15.99	8.41	7.68	4.79
90	8.03	8.22	12.13	9.53	9.50	6.31

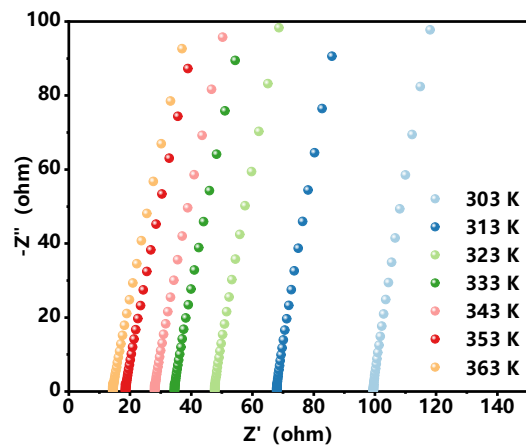


Fig. S6. EIS of DICPE-4 from 30 to 90 °C.

Table S3. Resistance and ionic conductivity of DICPE-4 at different temperatures

Temperature (°C)	Impedance (Ω)	Ionic conductivity (10^{-4} S cm $^{-1}$)
30	99.46	0.80
40	67.93	1.16
50	47.65	1.66
60	34.52	2.29
70	28.06	2.82
80	18.54	4.27
90	14.39	5.50

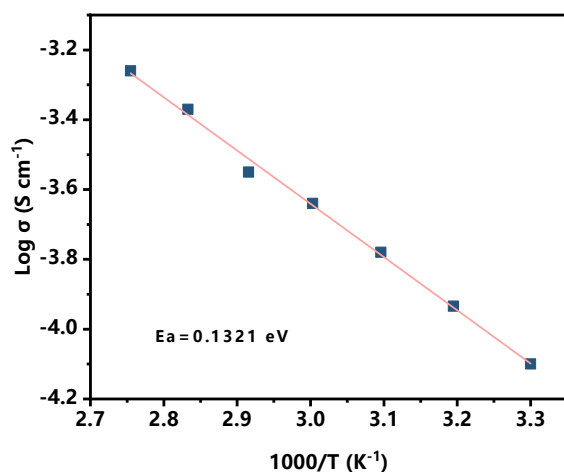


Fig. S7. Fitted Arrhenius curve of DICPE-4 membrane.

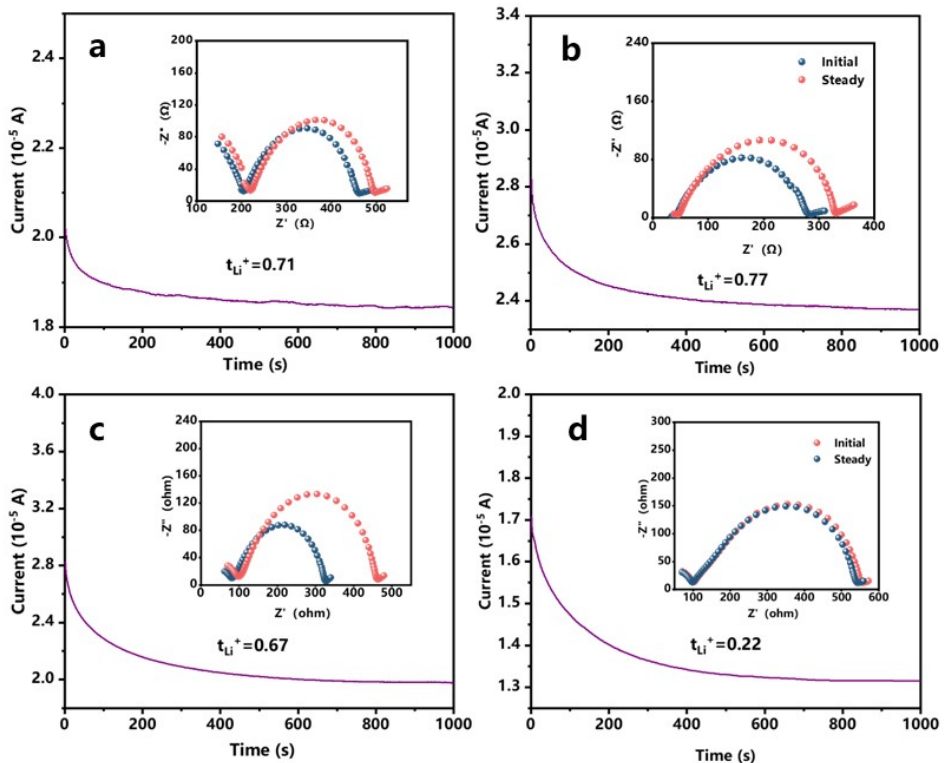


Fig. S8. Chronoamperometry profiles and impedance spectra (inset) before and after polarization for $\text{Li}||\text{Li}$ symmetric cells using (a) SICPE-2, (b) SICPE-4, (c) SICPE-6, and (d) DICPE-4.

Table S4. t_{Li^+} values of SICPEs and DICPE-4 at 25°C

	I_0	I_S	R_0	R_S	t_{Li^+}
SICPE-2	2.02×10^{-5}	1.84×10^{-5}	462	497	0.71
SICPE-4	2.82×10^{-5}	2.37×10^{-5}	284	330	0.77
SICPE-6	2.82×10^{-5}	1.98×10^{-5}	327	460	0.67
DICPE-4	1.71×10^{-5}	1.32×10^{-5}	544	556	0.22

Table S5. This work compares σ and t_{Li^+} with the reported PEs that using the LiSTFSI as monomer

Electrolyte composition	Ionic conductivity (σ)	t_{Li^+}	Ref.
poly(VEC10-r-LiSTFSI)	1.60 mS cm ⁻¹ at 20 °C	0.73	4
SIPPI	1 mS cm ⁻¹ at 30 °C	0.79	5
PL@LCSE	1.5 mS·cm ⁻¹ at 60 °C	0.77	6
SLIGPE-3.5	2.74×10^{-5} S cm ⁻¹ at room temperature	0.622	7
LPEDV-Li	4.7×10^{-5} S	0.94	8
PAEK-SIGPE	7.8×10^{-5} S cm ⁻¹ at 30 °C	0.95	3
SICPE-4	9.5×10^{-4} S cm ⁻¹ at 90 °C	0.77	This work

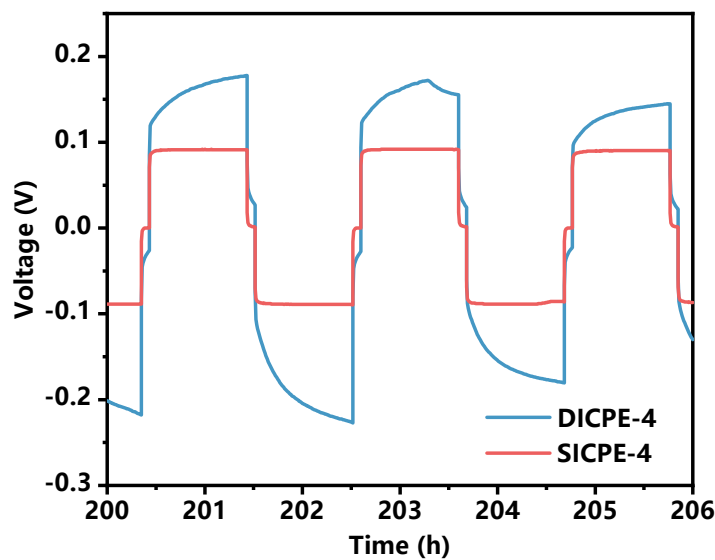


Fig. S9. Stripping/deposition curves of Li/SICPE-4/Li and Li/DICPE-4/Li batteries at a current density of 0.1 mA cm⁻².

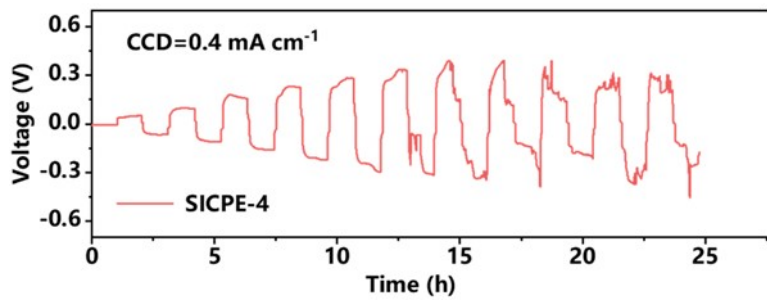


Fig. S10. Critical current density (CCD) of SICPE-4

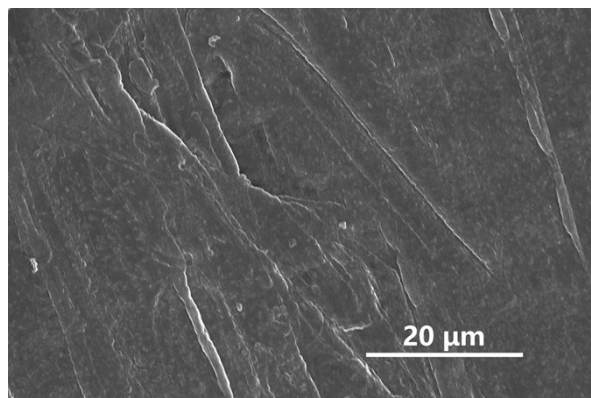


Fig. S11. SEM image of the lithium foil before cycling.

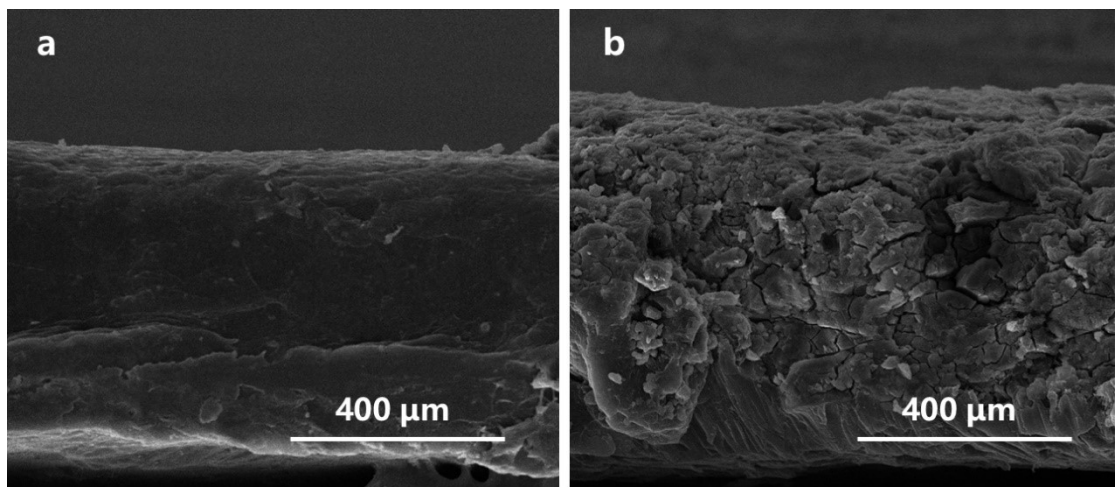


Fig. S12. Cross-sectional SEM images of Li metal anode from (a) SICPE-4 and (b) DICPE-4.

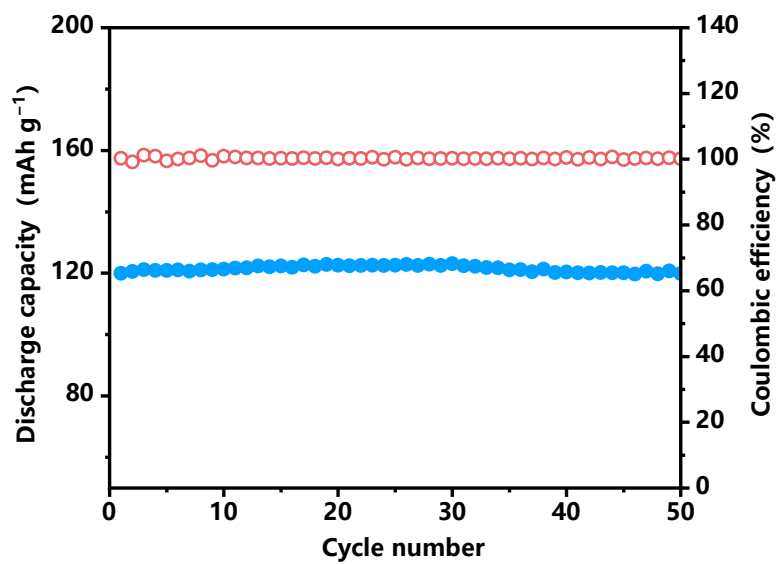


Fig. S13. Cycling performance and Coulombic efficiency of Li/SICPE-4/LFP at 0.5 C,
25 °C.

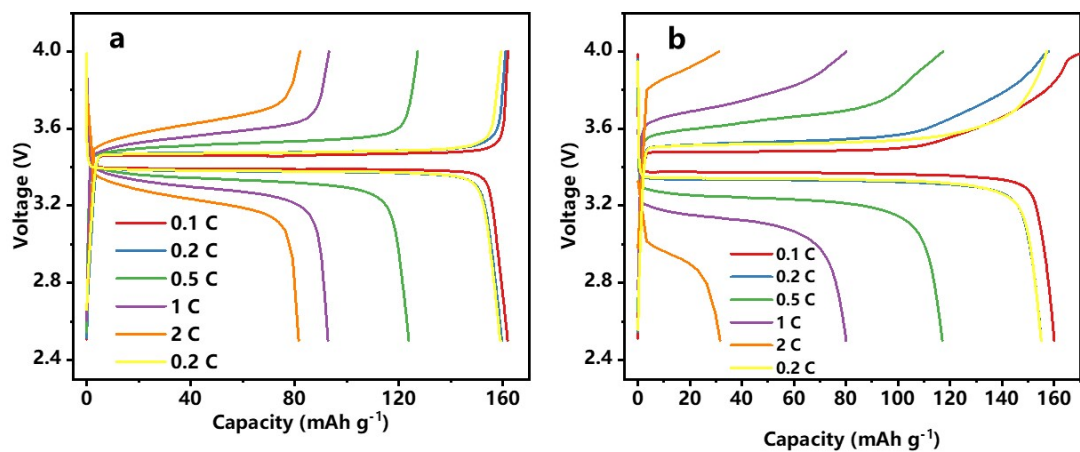


Fig. S14. Galvanostatic charge-discharge voltage profiles of the (a) Li/SICPE-4/LFP
and (b) Li/DICPE-4/LFP batteries under 0.1-2 C at 25 °C.



Fig. S15. Optical photograph of the thickness of the LFP positive electrode.



Fig. S16. Optical photograph of the thickness of the lithium metal anode.

References

1. T. Liu, L. Sun, R. Ou, Q. Fan, L. Li, C. Guo, Z. Liu and Q. Wang, *Chem. Eng. J.*, 2019, 368, 359-368.
2. R. Meziane, J. P. Bonnet, M. Courty, K. Djellab and M. Armand, *Electrochim. Acta*, 2011, 57, 14-19.
3. Z. Li, Y. You, X. Liang, P. Wang, Z. Zhang, X. Du, B. Liu, Z. Sun and W. Hu,

Appl. Surf. Sci., 2023, 611, 155363.

4. X. Shan, M. Morey, Z. Li, S. Zhao, S. Song, Z. Xiao, H. Feng, S. Gao, G. Li, A. P. Sokolov, E. Ryan, K. Xu, M. Tian, Y. He, H. Yang and P. Cao, *ACS Energy Lett.* 2022, 7, 4342–4351.
5. X. Shan, S. Zhao, M. Ma, Y. Pan, Z. Xiao, B. Li, A. P. Sokolov, M. Tian, H. Yang and P. Cao, *ACS Appl. Mater. Interfaces*, 2022, 14, 56110–56119.
6. M. Liu, X. Guan, H. Liu, X. Ma, Q. Wu, S. Ge, H. Zhang and Jun Xu, *Chem. Eng. J.*, 2022, 445, 1385-8947.
7. X. Guan, Q. Wu, X. Zhang, X. Guo, C. Li, J. Xu, *Chem. Eng. J.*, 2020, 382, 122935.

8. J. Zhang, Y. Zhong, S. Wang, D. Han, M. Xiao, L. Sun and Y. Meng, *ACS Appl. Energy Mater.*, 2021, 4, 862-869.